

## RESEARCH ARTICLE

10.1002/2016JD025130

## Special Section:

Studies of Emissions and Atmospheric Composition, Clouds and Climate Coupling by Regional Surveys, 2013 (SEAC4RS)

## Key Points:

- Wintertime ozone formation in a gas field
- Shallow, rapid photochemical ozone

## Supporting Information:

- Supporting Information S1

## Correspondence to:

R. C. Schnell,  
russell.c.schnell@noaa.gov

## Citation:

Schnell, R. C., et al. (2016), Quantifying wintertime boundary layer ozone production from frequent profile measurements in the Uinta Basin, UT, oil and gas region, *J. Geophys. Res. Atmos.*, 121, 11,038–11,054, doi:10.1002/2016JD025130.

Received 22 MAR 2016

Accepted 4 AUG 2016

Accepted article online 13 AUG 2016

Published online 19 SEP 2016

Published 2016. This article is a US Government work and is in the public domain in the USA.

## Quantifying wintertime boundary layer ozone production from frequent profile measurements in the Uinta Basin, UT, oil and gas region

Russell C. Schnell<sup>1</sup>, Bryan J. Johnson<sup>1</sup>, Samuel J. Oltmans<sup>1,2</sup>, Patrick Cullis<sup>1,2</sup>, Chance Sterling<sup>1,2</sup>, Emrys Hall<sup>1,2</sup>, Allen Jordan<sup>1,2</sup>, Detlev Helmig<sup>3</sup>, Gabrielle Petron<sup>1,2</sup>, Ravan Ahmadov<sup>2,4</sup>, James Wendell<sup>1</sup>, Robert Albee<sup>5</sup>, Patrick Boylan<sup>6</sup>, Chelsea R. Thompson<sup>3,4</sup>, Jason Evans<sup>3</sup>, Jacques Hueber<sup>3</sup>, Abigale J. Curtis<sup>3</sup>, and Jeong-Hoo Park<sup>3</sup>

<sup>1</sup>Global Monitoring Division, NOAA Earth System Research Laboratory, Boulder, Colorado, USA, <sup>2</sup>CIRES, 215 UCB, University of Colorado Boulder, Boulder, Colorado, USA, <sup>3</sup>INSTAAR, University of Colorado Boulder, Boulder, Colorado, USA, <sup>4</sup>Physical Sciences Division, NOAA Earth System Research Laboratory, Boulder, Colorado, USA, <sup>5</sup>Science and Technology Corporation, Boulder, Colorado, USA, <sup>6</sup>National Center for Atmospheric Research, Boulder, Colorado, USA

**Abstract** As part of the Uinta Basin Winter Ozone Study, January–February 2013, we conducted 937 tethered balloon-borne ozone vertical and temperature profiles from three sites in the Uinta Basin, Utah (UB). Emissions from oil and gas operations combined with snow cover were favorable for producing high ozone-mixing ratios in the surface layer during stagnant and cold-pool episodes. The highly resolved profiles documented the development of approximately week-long ozone production episodes building from regional backgrounds of ~40 ppbv to >165 ppbv within a shallow cold pool up to 200 m in depth. Beginning in midmorning, ozone-mixing ratios increased uniformly through the cold pool layer at rates of 5–12 ppbv/h. During ozone events, there was a strong diurnal cycle with each succeeding day accumulating 4–8 ppbv greater than the previous day. The top of the elevated ozone production layer was nearly uniform in altitude across the UB independent of topography. Above the ozone production layer, mixing ratios decreased with height to ~400 m above ground level where they approached regional background levels. Rapid clean-out of ozone-rich air occurred within a day when frontal systems brought in fresh air. Solar heating and basin topography led to a diurnal flow pattern in which daytime upslope winds distributed ozone precursors and ozone in the Basin. NO<sub>x</sub>-rich plumes from a coal-fired power plant in the eastern sector of the Basin did not appear to mix down into the cold pool during this field study.

### 1. Introduction

Recent observations have shown that high levels of photochemically produced surface ozone can occur in remote midlatitude locations during the winter in oil and gas production regions [Schnell et al., 2009; Oltmans et al., 2014; Edwards et al., 2014; Lyman and Tran, 2015]. The circumstances under which this wintertime ozone phenomenon has been observed include topographically constrained basins, snow-covered ground, strong and shallow temperature inversions, shallow boundary layers, and ozone precursor emissions from oil and gas extraction activities. The Upper Green River Basin in SE Wyoming and the Uintah Basin (UB) in NE Utah have exceeded the U.S. 2008 National Ambient Air Quality Standard (NAAQS) for ozone in multiple recent winters [Oltmans et al., 2014]. A number of winter research studies have been carried out in both of these locations [Utah DEQ, 2016; Wyoming DEQ, 2016]. Measurements presented here are from the 2013 Uinta Basin Winter Ozone Study [Stoetzenius and McNally, 2014], a multiagency, multi-institution study that took place under meteorological conditions that fostered significant surface ozone formation [Oltmans et al., 2014].

A previous study from 2012, in the Uinta Basin (UB) [Lyman and Shorthill, 2013] under snow-free winter conditions, found that while significant hydrocarbon emissions associated with oil and natural gas production were measured [Karion et al., 2013], including ozone precursor volatile organic compounds (VOCs) [Helmig et al., 2014; Warneke et al., 2014], this alone was not sufficient to produce elevated levels of ozone [Edwards et al., 2013] in the absence of snow cover and strong near-surface temperature inversions. Unlike 2012, the winter of 2013 was marked by significant snow cover throughout the UB [Oltmans et al., 2014].

In 2013, with a stable vertical air temperature structure [Neemann et al., 2015], surface emissions were trapped in a shallow boundary layer leading to high ambient levels of VOCs and nitrogen oxides (NO<sub>x</sub>)

[Helmig *et al.*, 2014]. The high surface albedo from the snow greatly enhances reflected upwelling solar radiation which accelerates photolytic ozone production.

A chemical box modeling study [Edwards *et al.*, 2014] suggested that substantial ozone production in the UB is facilitated under low reactive nitrogen oxide concentrations and high VOC concentrations where photolysis of carbonyl species produced by VOC oxidation played a dominant role in radical production.

Accurate modeling of cold-pool-like stagnant weather conditions and photochemistry in the UB poses several challenges [Baker *et al.*, 2011]. First, it is hard for meteorological models to simulate extremely stagnant weather conditions with very shallow daytime boundary layers and low wind speeds that last for several days. Second, traditional air quality models have been developed to simulate summertime ozone [Ahmadov *et al.*, 2015]. Third, the emissions of ozone precursors for the oil and natural gas sector in the inventory for the UB may not well represent actual emissions based on top-down estimates [Karion *et al.*, 2013; Ahmadov *et al.*, 2015].

These challenges were partly addressed by Ahmadov *et al.* [2015] using the state-of-the-art meteorology-chemistry Weather Research and Forecasting model coupled to Chemistry (WRF-Chem) to investigate photochemistry in the basin. They also estimated the emissions of ozone precursors from the oil and natural gas sector in the UB using NOAA's in situ measurements at the Horse Pool field site and total top-down methane emission estimate by Karion *et al.* [2013]. The modeling results suggested that the major factors driving high wintertime O<sub>3</sub> in the UB are the accumulation of O<sub>3</sub> precursors in shallow boundary layers with light winds, the NO<sub>x</sub> to VOC emission ratios from oil and natural gas operations, and the enhancement of photolysis fluxes and reduction of O<sub>3</sub> loss from deposition due to snow cover.

During the field work periods of January–March 2012 and 2013 natural gas production in the UB was nearly identical at ~2.5 trillion m<sup>3</sup>. Oil production from 1 January to 31 March 2013 was ~18% greater (~5.8 million barrels) than in 2012 [Utah Oil and Gas Program, 2015].

The main goals of the tetheredsonde research in the 2013 study were to (1) document the vertical and temporal distribution of the wintertime ozone production process, including the daily ozone growth rate, with high-resolution time/height measurements; (2) investigate the influence of surface wind patterns on ozone distribution in the UB; and (3) determine whether NO<sub>x</sub> emissions from the Bonanza power plant, located in the southeastern quadrant of the UB, are contributing precursors to the cold-pool surface layer during elevated ozone events.

## 2. Methods

### 2.1. Setting the Stage: Topography of the Uinta Basin Affecting Winter Ozone Formation

Figure 1a presents the locations of active oil (red dots) and natural gas (blue dots) wells in the UB along with sites mentioned in the paper. The UB (Figure 1b) is ringed by mountains, some in excess of 2100 meter above sea level (m asl). The lowest elevation in the basin is 1555 m asl in the Green River valley in the SSW of the basin. The boundary between the purple and turquoise contours in Figure 1b is at 1650 m asl which, as will be shown below, was the approximate altitude at the top of the cold-pool ozone production layer in winter 2013. As such, some of the oil wells in the western portion of the basin are in this transition zone between the ozone production layer and lower ozone air above. Figure 1 shows that ~50% (~5000 km<sup>2</sup>) of the area of the UB is below the 1650 m contour, which essentially encompasses the core wintertime ozone production zone observed during the 2013 campaign.

### 2.2. Ozone Measurements

During the winter of 2013, ozone data were collected using four complementary ozone measurement systems: (1) free-flying ozonesondes, (2) tethered balloon-borne combinations of radiosondes and ozonesondes profiling from the surface to above the boundary layer (up to 500 meter above ground level (m agl)) and back to the surface at three locations, (3) surface-based stationary ozone monitoring sites reporting data to the U.S. Environmental Protection Agency (EPA), and (4) ozonesondes mounted on vehicles driven in the UB. The data collected and processed in this project are freely available (Uinta Basin Ozone Project, see <ftp://aftp.cmdl.noaa.gov/data/ozwv/Ozonesonde/Field%20Projects/Uintah/UINTAH%202013/>) on a NOAA website/ftp server and at (<http://www2.epa.gov/aqs>).

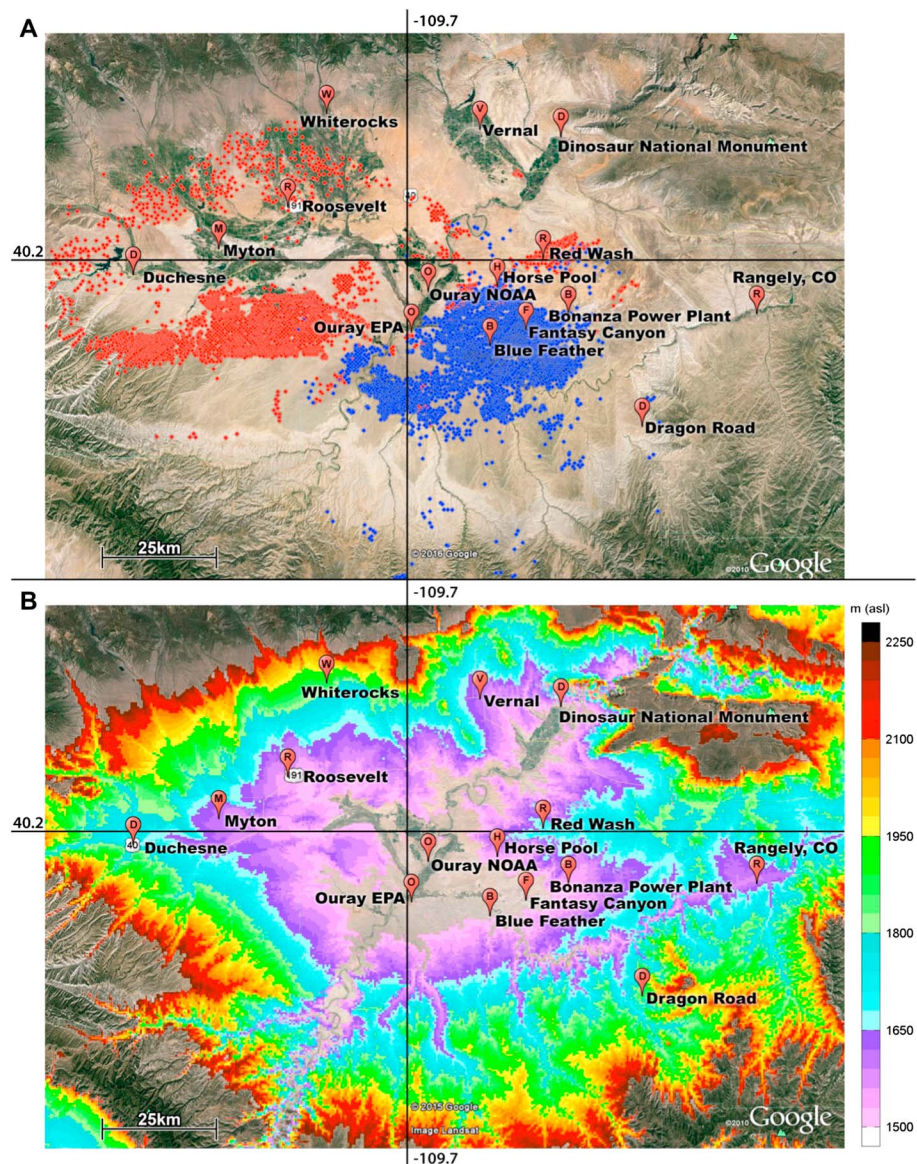


**Figure 1.** Uinta Basin oil and gas wells and topography maps. (a) Uinta Basin tethered ozone locations (Ouray, Horse Pool, and Fantasy Canyon) along with surface ozone monitoring locations. Gas well locations are shown as blue dots and oil well locations as red dots. (b) Topography in the Uinta Basin. The boundary between the purple and turquoise color corresponds to the 1650 m asl elevation contour, which was the average top of the cold-pool layer ozone production zone during the 30 January to 8 February ozone production event.

### 2.2.1. Ozonesondes

Supporting information Table S1 lists the specifications for the ozonesonde and surface ozone instruments used in 2012 and 2013. The ozonesonde measurement precision was  $\pm(3\text{--}5)\%$  with accuracy of  $\pm(5\text{--}10)\%$  up to 30 km altitude, based on environmental chamber simulation tests [Smit *et al.*, 2007] and a field ozonesonde campaign [Johnson *et al.*, 2008]. The ozonesondes were interfaced with iMet radiosondes, which measure and transmit ambient pressure, temperature, relative humidity, and GPS altitude, latitude, and longitude along with the ozone data.

### 2.2.2. Tethered Ozonesondes (Tethersondes)

The NOAA ozonesonde tether system used at Ouray and Fantasy Canyon is a custom-made device based on a motorized deep-sea fishing rod and reel with a 50 pound line (Figure S1 in the supporting information). The design includes communication software, and data loggers operated from a laptop computer to continuously monitor the radiosonde pressure, allowing control of the ascent and descent rates. Ozone, temperature,

and humidity are radioed to the surface in real time along with GPS altitude, latitude, and longitude of the instrument package. Wind direction (but not speed) was derived from the balloon heading provided by the GPS. A normal ascent and descent profile pair was completed once per hour to heights of up to 325 m agl (above ground level). At Horse Pool, the group from the Institute of Arctic and Alpine Research (INSTAAR), University of Colorado, operated an analogous tethered system with a larger winch system capable of operating ozonesondes to 500 m agl.

The ozonesondes were conditioned and prepared according to NOAA Global Monitoring Division standard operating procedures, and at Ouray compared for 3 min prior to and following each profile to a NIST-standardized Thermo Environmental (TEI Model 49C) UV surface ozone monitor operated continuously at the site. For Fantasy Canyon, each sonde was compared prior to and subsequent to the day's operation with the same Ouray-based ozone monitor. Comparison of ozone-mixing ratios measured by the tethered ozonesondes and the Ouray TEI showed an  $R^2$  of 0.9959 (Figure S2).

Ozone-mixing ratio and temperature profiles were measured between 24 January and 7 February 2013 at the Ouray Wildlife Refuge (hereafter Ouray) and at Fantasy Canyon by NOAA, and at Horse Pool by INSTAAR from 25 January to 19 February 2013. During the campaign altogether 937 vertical profiles of ozone, temperature, relative humidity, and wind direction were obtained.

### 2.2.3. Surface Ozone and NO Measurements at Fixed Locations

Continuous measurements of surface ozone-mixing ratios were obtained by NOAA at the Ouray tethered site with a TEI UV absorption ozone monitor. At Horse Pool, surface ozone data were obtained by the INSTAAR group using a TEI 49i ozone monitor. This report also uses hourly average surface ozone data from the EPA, National Park Service, and other ozone monitoring stations equipped with either Teledyne API 400E or TEI Model 49 ozone monitors. These data are available from the EPA Air Quality System (AQS) site. The NOAA and INSTAAR monitors were calibrated against a NIST traceable standard prior and subsequent to deployment and have an accuracy of  $\pm 1$  ppbv, and a precision of better than  $\pm 3\%$  (Table S1). The EPA/AQS sites follow their own quality assurance protocols specified by the EPA. NO data were also obtained from the EPA AQS site. These data were primarily used to show differences between locations distributed across the basin.

### 2.2.4. Vehicle Mounted Mobile Ozonesonde Measurements

Each day of the study period ozone was measured with sondes mounted in the window openings of vehicles driving through the basin at highway speeds passing within 2 km of the Red Wash and Blue Feather ozone monitors. In 16 drive-by comparisons, the 10 s average mobile ozone measurements were on average 0.75 ppbv (standard deviation of 2.8 ppbv) lower than the hourly averaged Red Wash and Blue Feather measurements. On 6 February 2013, ozone was measured on a drive up the south rim of the basin passing through the top of the cold-pool temperature inversion and then back down into the ozone production layer.

## 2.3. Surface Wind Measurements

To further investigate the atmospheric conditions impacting the spatial and temporal distribution of surface ozone during the campaign, we used hourly averaged meteorological data collected from eight EPA AQS monitoring sites in the basin. At the sites, horizontal wind speed and direction were measured at the same height as ozone. The wind data are displayed as wind roses in 22.5° sectors and divided into "day" (1000–1500 MST) and "night" (1600–0900 MST) time windows. The winds were composited for two episodes of high surface ozone-mixing ratios, 20–26 January and 1–6 February 2013.

## 3. Results

### 3.1. Meteorology of the 2012 and 2013 Ozone Production Events in the Uinta Basin

During the 2012 winter study, there was relatively warm weather and an absence of snow cover. No cold-air pooling events developed under these conditions, as there were no strong multiday, near-surface temperature inversions. During daytime in 2012, a 10 to 15 ppbv increase in surface ozone was observed, with daytime maxima, typically in the 45 to 55 ppbv range [Lyman and Shorthill, 2013]. Nighttime ozone levels were 30 to 40 ppbv. The presence of persistent snow cover (Figure S3), as well as synoptic conditions that produced stagnation in the basin denotes the crucial difference in the meteorology controlling ozone formation in 2013. The averaged morning and afternoon profiles measured at Ouray clearly depict the contrast between 2012

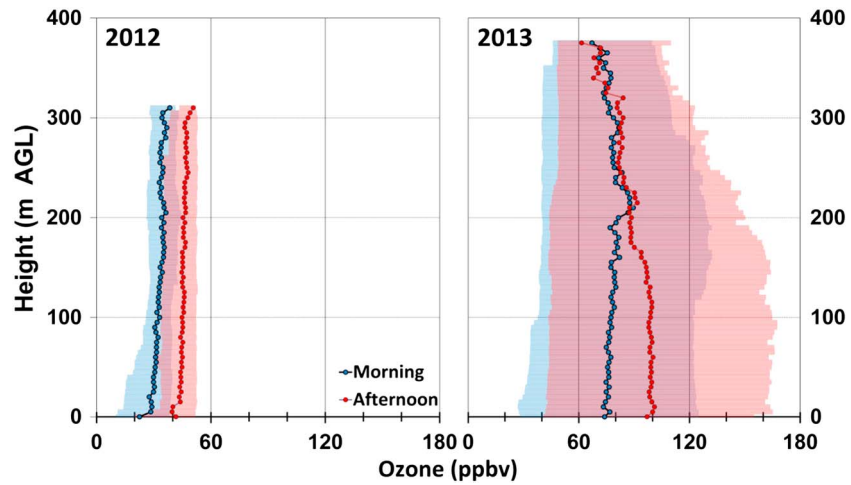


**Figure 2.** Summary plot of 2012 and 2013 tethered-sonde-mixing ratios at Ouray. The average ozone-mixing ratios and minimum and maximum measured at Ouray during morning (between sunrise and local noon, in blue) and afternoon (noon to sunset, in red) for the 2012 (54 profiles) and 2013 (167 profiles).

and 2013 ozone production (Figure 2). In 2012, ozone increased by only a few ppbv from morning to afternoon, and the increase in ozone was essentially constant with altitude up to 300 m agl. In 2013 at Ouray, we measured ozone levels up to 160 ppbv near the surface in the afternoon on a number of occasions.

**3.2. Surface Ozone**

Hourly average surface ozone in various portions of the basin measured between 15 January and 15 February 2013 at eight sites (Table 1) is presented in Figure 3. The dots on the ozone concentration traces are the EPA regulatory 8 h average ozone mixing ratios and the red horizontal line the level above which the sites were in regulatory exceedance above the 2008 NAAQS for 8 h average ozone. A diurnal ozone cycle and ozone buildup over time is in clear evidence with successive daytime values generally greater than those during the previous day. Ozone-mixing ratios built up evenly over ~5000 km<sup>2</sup> in the UB within the cold pool until episodes concluded with sudden (as on 27 January) or more gradual (as on 7–10 February) drops in ozone.

**Table 1.** Uinta Basin Tethered Ozonesonde and Surface Site Locations, Number of Profiles Measured and Maximum Ozone-Mixing Ratios Measured in 2012 and 2013

Location	Longitude (°W)	Latitude (°N)	Elevation (m)	# of Tether Profiles/Dates	[O <sub>3</sub> ] 1 h Max Average (ppbv) <sup>a</sup>
2012 Tethersonde sites					
Ouray (NOAA)	109.644	40.134	1430	42/6–27 Feb	54
Horse Pool	109.467	40.143	1569	68/ 7–26 Feb	59
Jensen	109.351	40.368	1454	33/6–28 Feb	47
Roosevelt	110.008	40.294	1587	8/16 Feb	51
2013 Tethersonde sites					
				Total: 145	
Ouray	109.644	40.134	1430	387/24 Jan to 7 Feb	167
Horse Pool	109.467	40.143	1569	203/24 Jan to 17 Feb	162
Fantasy Canyon	109.394	40.058	1470	132/31 Jan to 7 Feb	152
2013 Surface sites					
				Total: 732	
Ouray (NOAA)	109.644	40.134	1430	24 Jan to 15 Feb	141 <sup>a</sup>
Ouray (EPA)	109.688	40.057	1464	15 Jan to 15 Feb	155
Blue Feather (NOAA)	109.484	40.025	1489	2 Feb to 15 Feb	133
Red Wash (EPA)	109.352	40.197	1689	15 Jan to 15 Feb	134
Vernal (UDAQ)	109.510	40.452	1606	15 Jan to 15 Feb	121
Dinosaur NM (NPS)	109.305	40.437	1463	15 Jan to 15 Feb	130
Horse Pool (INSTAAR)	109.467	40.143	1569	26 Jan to 15 Feb	146
White Rocks (EPA)	109.907	40.484	1893	22 Jan to 15 Feb	121
Myton (EPA)	110.183	40.217	1606	22 Jan to 15 Feb	126
Rangley (NPS)	108.762	40.087	1648	15 Jan to 15 Feb	120
Dragon Road	109.097	39.869	1879	15 Jan to 15 Feb	128

<sup>a</sup>Tethersonde maximum ozone is a ten second average, surface sites maximum ozone is an hourly average

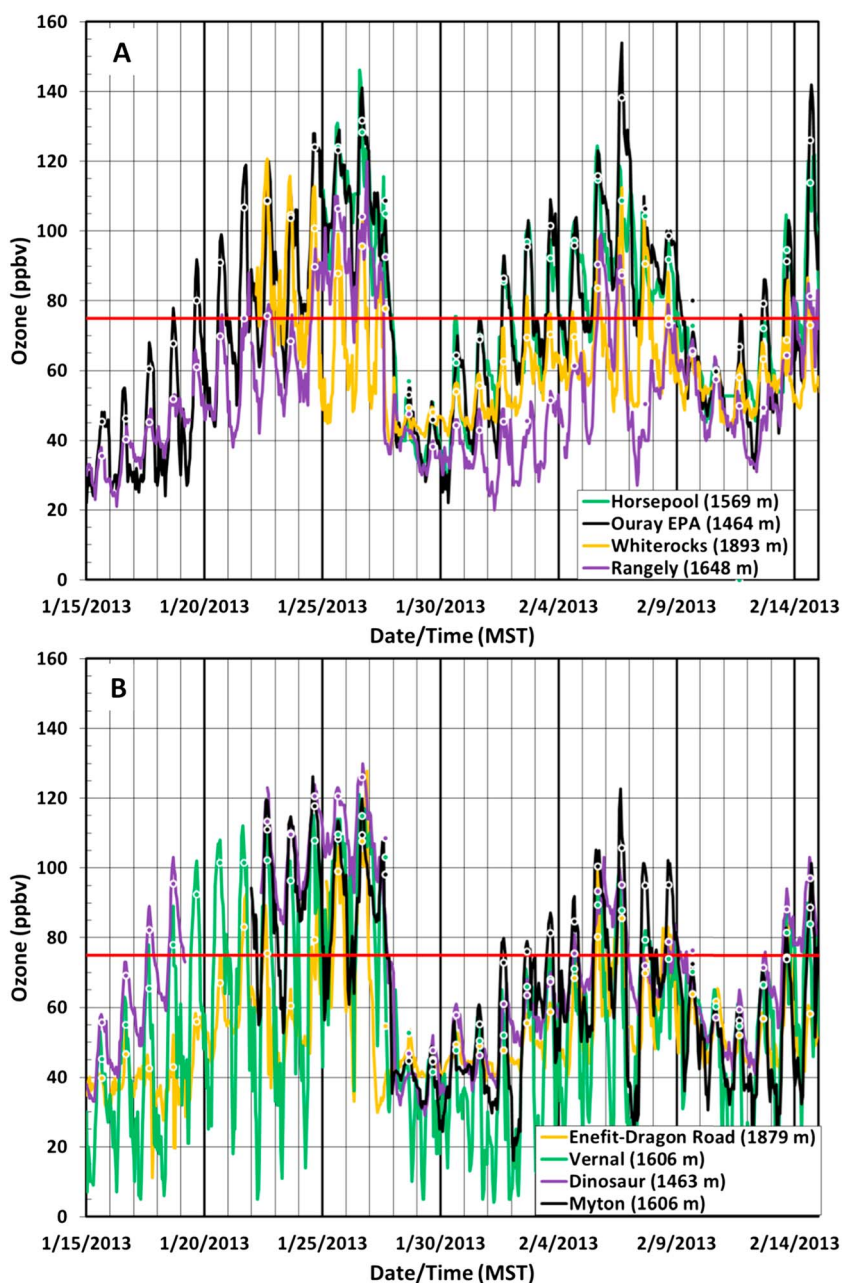


**Figure 3.** Surface hourly averaged ozone-mixing ratios across the Uinta Basin for (a) Horsepool, Ouray, Whiterocks, and Rangely and (b) Enefit-Dragon Road, Vernal, Dinosaur, and Myton showing the diurnal variation, buildup, and subsequent clean-out during the period of tether-sonde measurements. Dinosaur and Rangely in upriver locations are well removed from the gas fields. Note the nighttime titration of ozone in the urban center of Vernal (green trace). The red horizontal line indicates the 75 ppbv 2008 8 h average NAAQS for ozone and the circled dots the 8 h average for each day.

Clean-out events occurred during frontal passages when fresh air from outside the basin flushed out the ozone and ozone precursor-rich surface air (see Figure S4 and Neemann *et al.* [2015]).

The day-to-day buildup of the daytime maxima implies that the nightly ozone loss via chemical loss, surface deposition, and mixing out of the boundary layer does not compensate for the daytime ozone production, except at Vernal (1606 meter above sea level (m asl), 60 km from the gas field) on the north side of the basin. At Vernal (Figure 3b, green trace) nighttime surface ozone levels regularly dipped to lower levels (occasionally to < 5 ppbv), much lower than observed at the other sites, even as overall daily maximum ozone-mixing ratios continued to increase. The probable cause of this nighttime ozone titration with the high nocturnal

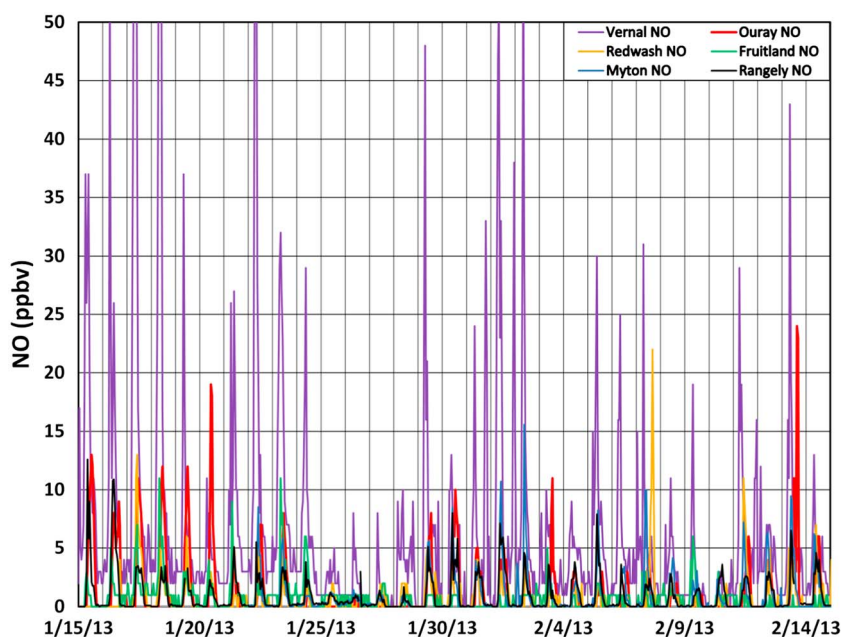


**Figure 4.** NO concentrations measured at six sites around the Uintah Basin during three ozone production episodes. Note the high nighttime NO concentrations measured at Vernal, and elevated but relatively lower concentrations at Ouray.

NO concentrations observed in Vernal (purple trace) compared to the other sites around the basin (Figure 4). This suggests NO titration of ozone was stronger at this site, possibly from vehicle traffic that continues through the night in the Vernal industrial hub.

A basin-wide production/distribution of ozone is further supported by the elevated ozone observed (Figure 3) at the edges of the basin, such as at Rangely, Colorado (elevation 1648 m asl), at the eastern extent of the basin and in the north at Dinosaur National Monument (1463 m asl). Both locations are  $>50$  km away from the gas field. The ENFIT/Dragon Road monitor on the southeastern flank of the basin recorded high ozone-mixing ratios only on the last 2 days of the late January episode and 1 day near the end of the early February episode. This ozone monitor (1879 m asl) is on most occasions at an elevation higher than the  $\sim 1650$ – $1750$  m agl top of the ozone producing cold pool within the basin during this study period.

### 3.3. Mobile Surface Ozone Measurements

Ten second averaged data from a van drive through the basin on 6 February 2013 are presented in Figure 5 for surface ozone-mixing ratio and temperature (left axis) and surface elevation above sea level (right axis) against time. Gaps in the data occur when the van was stopped, thus preventing adequate ventilation of the ozone and temperature sensors. Ozone-mixing ratios were  $\sim 75$  ppbv when leaving Vernal (location 1) at  $\sim 1300$  MST, rising to 115 ppbv in the Green River valley (location 2,  $\sim 1450$  m asl), decreasing to 90 ppbv near the Red Wash EPA ozone station (location 3), where the elevation of the road was high enough (1720 m asl) such that the van was in the transition zone near the top of the inversion layer. When the elevation of the road decreased again, the ozone-mixing ratio increased to 143 ppbv just prior to 1500 MST in a valley (elevation 1495 m asl) between locations 4 and 5 in Figure 5.

Ozone peaked again at 143 ppbv (just past location 7) at 1600 m asl as the van began an ascent up the south wall of the basin at which point ozone began to steadily decrease as temperature ( $\sim -4.8^\circ\text{C}$  at that location) steadily increased with elevation. At  $\sim 1985$  m asl, at location 8 (just before 1700 MST), ozone-mixing ratios were in the 50 ppbv range indicating the van was above the temperature inversion. The temperature at location 8 was  $\sim +2^\circ\text{C}$ , an increase of  $\sim 7^\circ\text{C}$  over an elevation gain of 385 m, whereas ozone decreased by  $\sim 93$  ppbv over the same elevation change.

The temperature and ozone patterns essentially repeated in reverse on the descent. It is interesting to note that the ozone-mixing ratio of  $\sim 100$ – $105$  ppbv (location 3), in the northern portion of the basin at 1700 m asl, was about the same as at 1700 m asl on the southern slope of the basin (between locations 7 and 8) separated

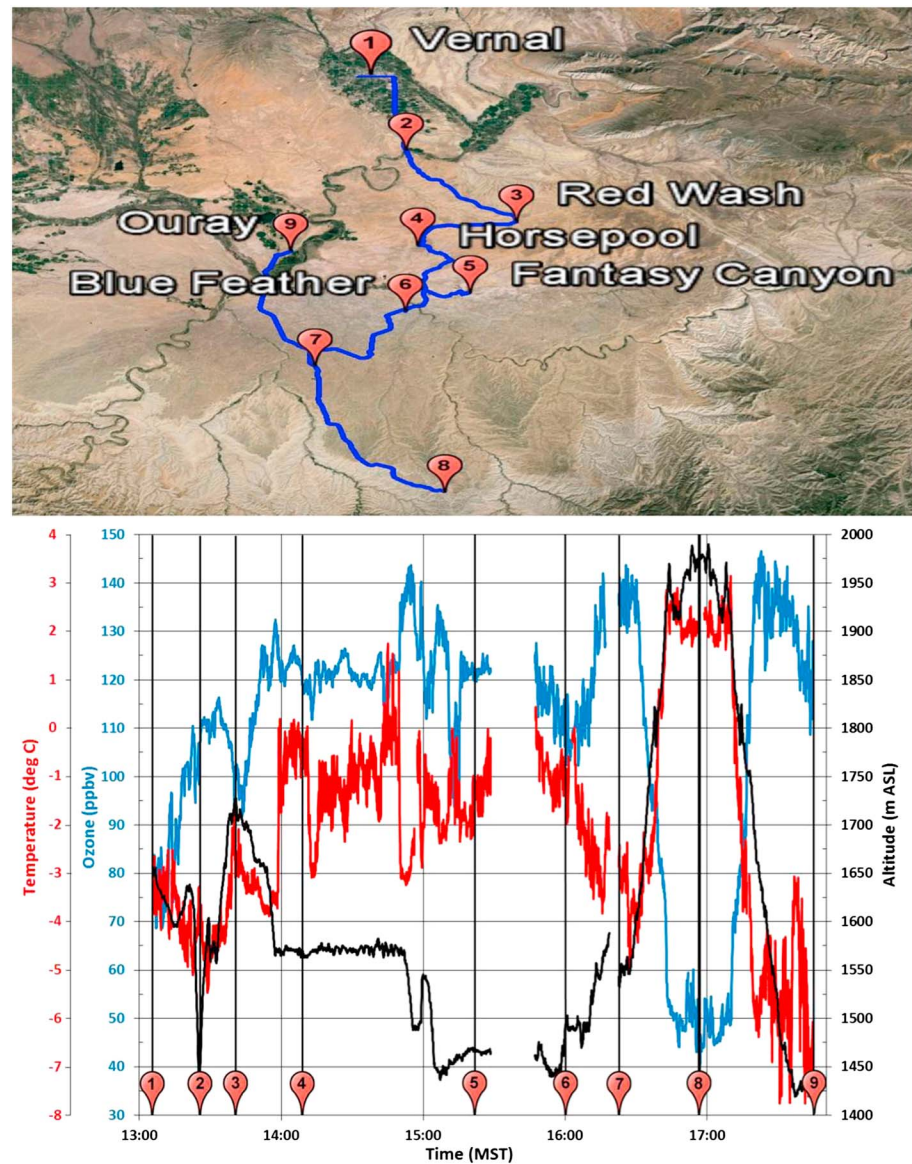


**Figure 5.** Ozone and temperature on a transect up the south slope of the Uinta Basin. Surface ozone and temperature plotted against altitude over time on a drive beginning in Vernal through the eastern portion of the Uinta Basin and up the south rim of the Uinta Basin through the top of a temperature inversion at  $\sim 1700$  m asl on 6 February 2013. Note how ozone decreases with height between points 7 and 8 while temperature increases within the inversion transition zone.

by 50 km and  $\sim 3$  h. This supports other observations presented in this paper that the top of the elevated ozone production layer is near the same altitude across the basin, independent of surface topography. These data reinforce the observation that the cold pool is a local phenomenon, which isolates the basin from the outside and traps local emissions leading to the production and accumulation of surface ozone as presented earlier. Plots from other drives are available at *Uinta Basin Mobile Measurements* [2016].

### 3.4. Ozone Vertical Structure from Tethersonde Data

Tethersonde profiles of ozone and potential temperature (10 s averages) for the 26 January to 6 February event measured at Ouray, Fantasy Canyon, and Horse Pool for near coincident times are presented in Figure 6. The profiles are afternoon soundings when ozone had built up to near peak mixing ratios for the day. On 26 January (Figure 6a) elevated ozone-mixing ratios extended to an altitude of  $\sim 1650$  m asl, which coincides with the top of the cold pool. On 30 January (Figure 6c) there was a cold, near isothermal temperature layer ( $\sim -11.5^\circ\text{C}$ ) between the surface and 1600 m asl, above which temperatures were  $5^\circ\text{C}$

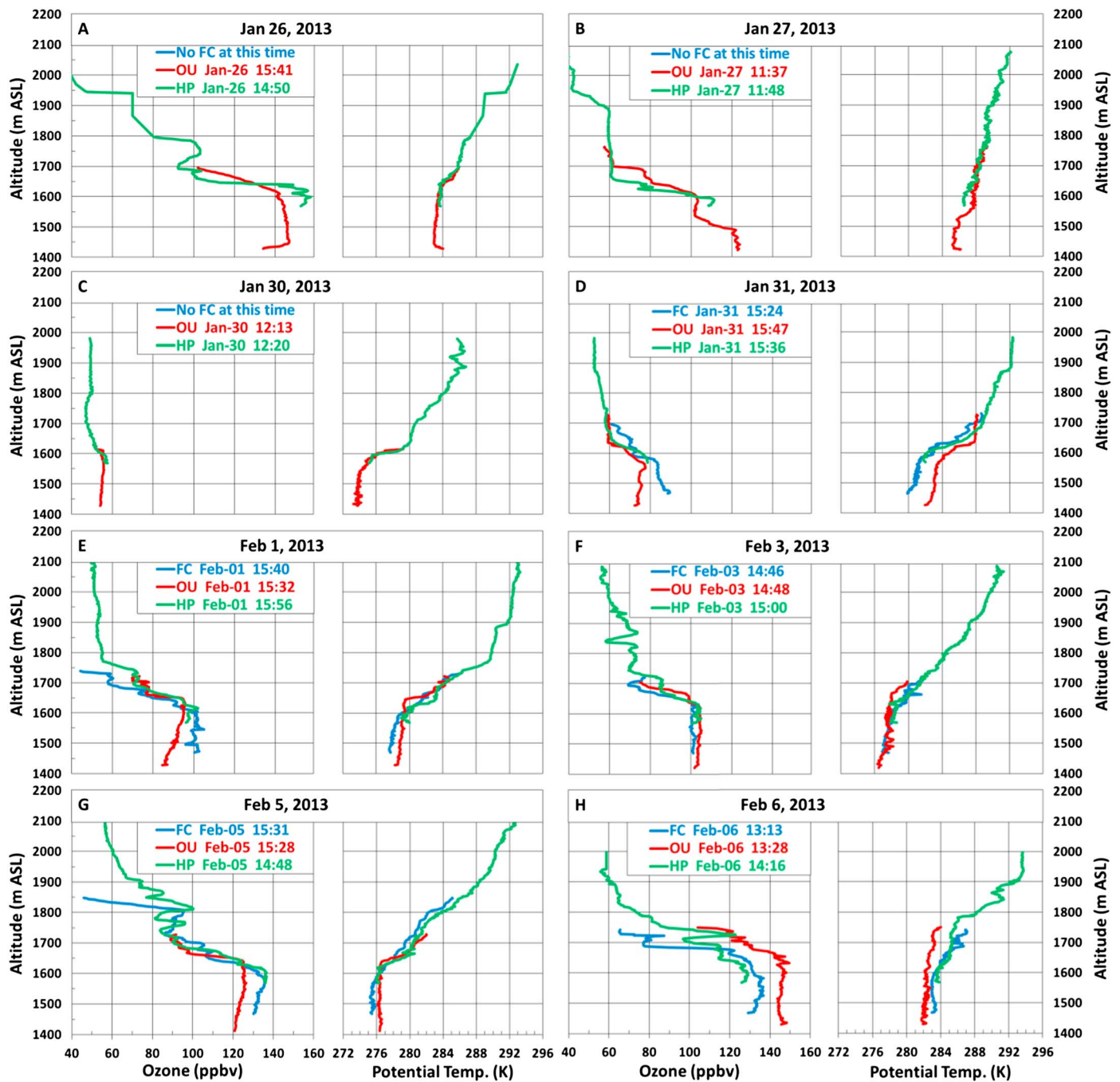


**Figure 6.** Coincident ozone and temperature profiles from three dispersed locations. (a–h) Profiles measured at Fantasy Canyon (FC, blue), Ouray (OU, red), and Horse Pool (HP, green) on selected days between 26 January and 6 February. Times are mountain standard time (MST).

warmer. Two days later, on 1 February, (Figure 6e) the top of the cold pool remained at ~1600 m asl. All three tetheredsonde sites had ozone-mixing ratios of 85–100 ppbv on 1 February within the cold pool, gradually decreasing to 50–70 ppbv, and 100–150 m above the top of the cold pool.

Daily ozone-mixing ratios continued to increase (Figures 6f and 6g) over the next 5 days with peak ozone attaining 147 ppbv on 6 February (Figure 6h) at Ouray. On 6 February, an ozone transition layer extended to ~1700 m asl. A striking feature in all the profiles is the uniform altitude of the top of the cold layer at each of the three sites indicating that the top of the layer was relatively uniform (as opposed to terrain following) over the portion of the basin encompassed by the tetheredsonde sites. Data in Figure 6 (green profiles) show

that at Horse Pool (1569 m asl) the elevated ozone layer varied from 50 m to 100 m deep, while at Ouray (1430 m asl) the elevated ozone layer was ~200 m deep. The height of a typical oil or gas drilling rig used in the UB is 50 m. As such, a rig drilling near Horse Pool would, on occasion, poke through the top of the ozone-rich, cold-pool layer. As was shown in Figure 5, it was possible to drive up a highway on the south rim of the basin to well above the cold-pool ozone layer.

At Horse Pool, the tethersonde profiles began near sunrise which was ~0730 MST. These early-morning profiles can be compared with the earliest profiles at the other two tethersonde sites that normally began measurements about 1 to 2 h later. Based on the comparison with early-morning Horse Pool soundings, the ozone buildup at Ouray and Fantasy Canyon did not begin until about the time of the initial soundings at these sites, which was 0830–0930 MST with the peak generally occurring at all three sites between 1400 and 1500 MST.

#### 3.4.1. Ouray Ozone Profile Cross Sections

At the Ouray and Fantasy Canyon sites, on average, four tethersonde ozone profiles per hour were obtained over an 8 h period (~32 per day). This allowed for high time/height resolution of the ozone production process as presented in Figure 7 for Ouray on selected days between 26 January and 6 February 2013. In Figure 7a it may be observed that in the early morning of 26 January ozone-mixing ratios were ~100 ppbv in a shallow layer near the surface and built up continually into the midafternoon through the lowest 150 m agl, reaching 160 ppbv between 1500 and 1600 MST. This elevated ozone episode was followed by a basin clean-out that lasted to 30 January.

Following the clean-out, late in the afternoon on 30 January (Figure 7c), a buildup of ozone was beginning in a layer up to ~1650 m asl with ozone-mixing ratios attaining 75–80 ppbv between 1600 and 1700 MST. On subsequent days (Figures 7d and 7e) ozone-mixing ratios continued to increase reaching >160 ppbv between 300 and 1500, MST 6 February. On each succeeding day during the ozone buildup, early-morning ozone concentrations were generally higher than on the previous morning and showed a fairly uniform development of the ozone-rich layer within the cold pool beneath the temperature inversion. In the early evening of 6 February air with lower ozone-mixing ratios (70–80 ppbv) began moving into the basin from the west.

Figure S5 illustrates details of the ozone development from selected individual ozone profiles through the day on 6 February 2013 above Ouray. From the ~100 ppbv ozone-mixing ratio at 1009 MST (red profiles) ozone built up through the day to >165 ppbv by 1350 MST in the afternoon. Mixing ratios subsequently decreased rapidly (blue profiles), starting at higher altitudes as the ozone-rich air was replaced by low ozone air as a frontal system began to enter the basin (Figure S4).

#### 3.4.2. Horse Pool Ozone Profile Cross Sections

At Horse Pool, tethersonde profiles were obtained from 25 January to 18 February 2013 with late night and early-morning soundings that allowed for the production of a continuous cross section with limited interpolation over periods of no data encompassing three high ozone episodes (Figure 8). While the basic features of each episode exhibit strong buildup of ozone followed by a rapid flushing, each episode had unique characteristics. The first episode beginning on ~18 January (from surface data) and ending on 28 January had the longest period of sustained high ozone-mixing ratios of the three episodes shown in Figure 8.

The second ozone event in the first week of February occurred in a shallower boundary layer than the prior event in late January. The clean-out of this event occurred over several days. In these two episodes the upper boundary of the highest ozone-mixing ratios was generally at ~1700–1750 m asl. However, the layer above ~1750 m asl was quite variable in both depth and steepness of the gradient from the enhanced ozone layer up to regional background levels in the free troposphere.

The Horse Pool tethersonde data occasionally indicate segments of low ozone at heights of 1750–2000 m asl as outlined with black boxes in Figure 8. We attribute these observations to occasions when the tethersonde intersected the Bonanza power plant plume. Within the plume, elevated SO<sub>2</sub> interferes with the chemistry of the ozone sensors, causing them to register artificially low ozone levels [Schenkel and Broder, 1982], and NO titration within the plume also produces low ozone-mixing ratios [Luria et al., 1999, 2003]. The lack of night soundings at Ouray and Fantasy Canyon did not allow plotting a similar cross section for either of these sites.

#### 3.5. Free-Flying Ozonesonde Profiles

Two standard balloon release ozonesondes were launched from Ouray during ozone events on 25 January at 1708 MST and on 7 February at 1440 MST (Figure 9). These profiles provide additional evidence of a boundary

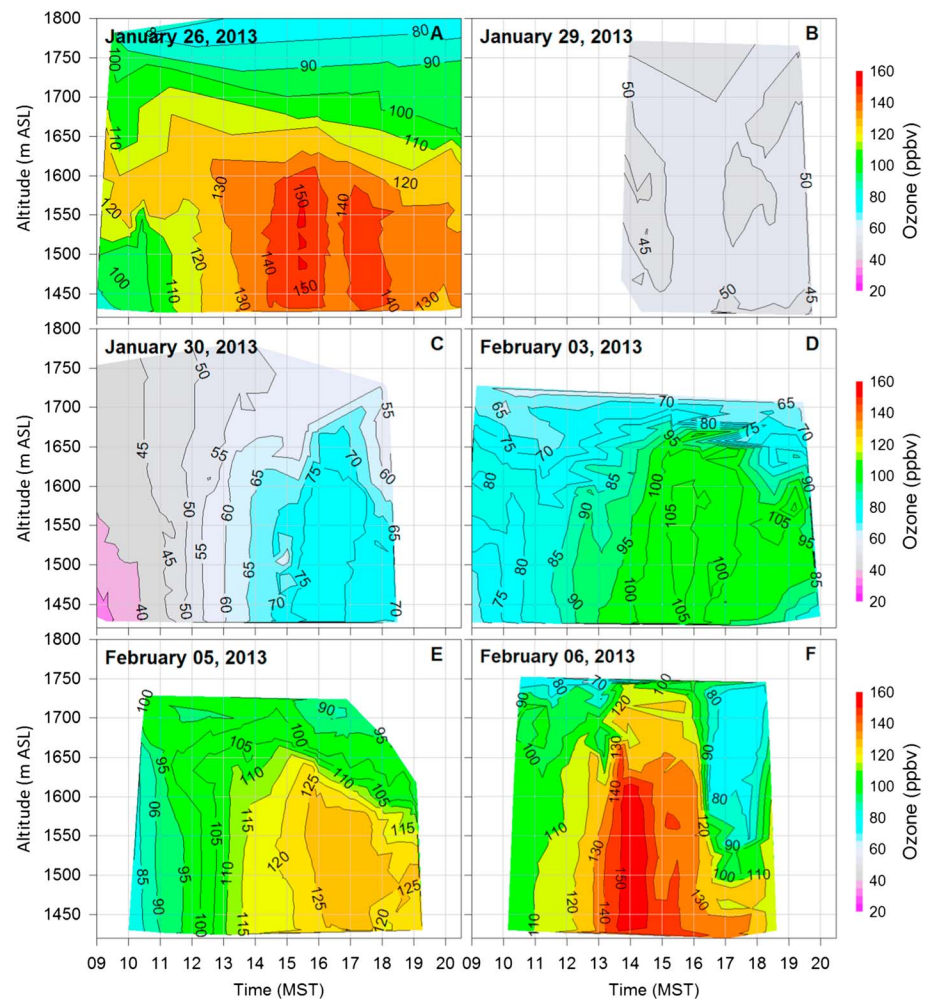


**Figure 7.** Ozone-mixing ratio cross sections through an ozone production event. A sequence of ozone-mixing ratio (ppbv) time-height cross sections for the period 26 January to 6 February 2013 from the tethersonde profile measurements at Ouray. (a–f) Data from 350 separate profiles are represented. The clean-out on 29 January and the intense ozone production on 6 February are standout features.

layer origin for the high ozone-mixing ratios as the near-surface, elevated mixing ratios are confined to the lowest 200 m asl. Throughout the troposphere, the mixing ratios were in the range 50–60 ppbv (free-troposphere regional background). Only when the balloons entered the stratosphere did ozone-mixing ratios exceed those measured near the surface.

### 3.6. Surface Winds Distributing Ozone Precursors and Ozone Across the Basin

The wind pattern at Whiterocks on the northern slope of the Basin and at Rangely on the east slope is presented in Figure 10. Data for stations on the other slopes of the Basin during the high ozone production events of 22–26 January and 1–7 February 2013 are provided in Figure S6. The locations of the stations were presented in Figure 1, and Table 1 gives their coordinates and elevations. The wind patterns observed in the basin conform to those expected from daytime upslope movement of air from daytime heating and nighttime cool air drainage toward lower elevations [Whiteman *et al.*, 1989; Lehner *et al.*, 2011]. This first-order study of UB winter winds shows that there is a diurnal process for moving ozone precursors and ozone from the interior of the basin toward the edges during the day as presented earlier in Figure 3. This is further supported by observations that upslope winds helped raise the hourly average ozone concentrations at Dinosaur National Monument, located in a pristine valley 70 km from the center of the gas field, to 128 ppbv on 26 January 2013 by 1400, and to 120 ppbv in Vernal, 60 km from the gas field at about the same time (Figure 3b).

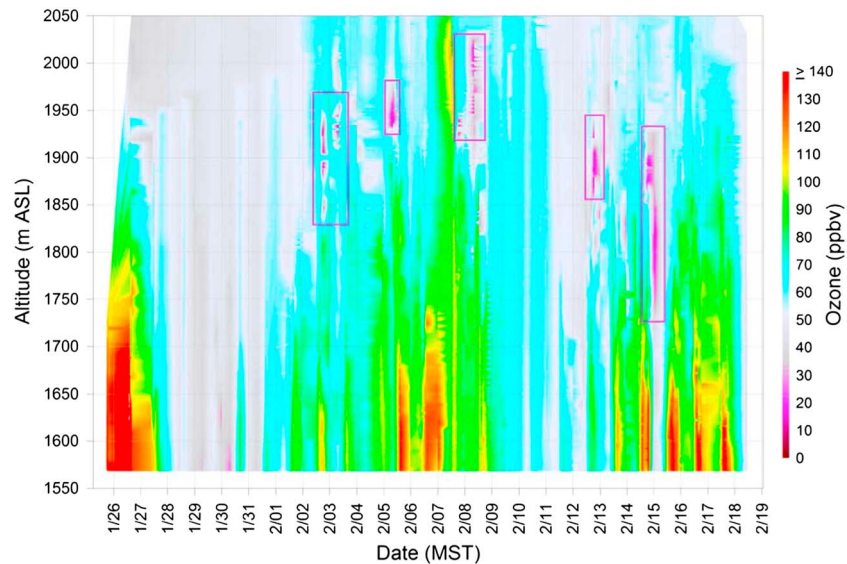


**Figure 8.** Horse Pool tethered-sonde ozone contour plot for 25 January to 18 February 2013. Time-height cross section of ozone-mixing ratios at Horse Pool showing three ozone production events and two intervening clean-outs. Occasions with depleted ozone boxed in purple are caused by SO<sub>2</sub> interference and NO titration of ozone when the tethered-sonde is in the Bonanza power plant plume.

### 3.7. Ozone Production and Destruction Rates at Ouray and Fantasy Canyon

The daily buildup of ozone in the UB, as a function of altitude, was quantified using the sequence of ozone profiles throughout the day at Ouray and Fantasy Canyon. Ozone measured within a 5 m band in profiles centered on 50, 100, 150, 200, and 250 m was averaged to obtain a value for that level and plotted against the time the sonde passed through the center of the respective levels as presented for Ouray in Figure 11. The ozone-mixing ratios from the colocated continuous ozone monitor are plotted in green at the 2 m level, the height of the sample inlet.

The average growth rates for all days at Ouray and Fantasy Canyon are presented in Table 2. As in Figure 11 for Ouray, the continuous surface ozone measured at the surface and the corresponding ozone-sonde mixing ratios measured at the same 2 m agl level at Ouray and Fantasy Canyon on all days were in excellent agreement. On 6 February at Ouray, the ozone growth exceeded 11.2 ppbv/h at all heights up to

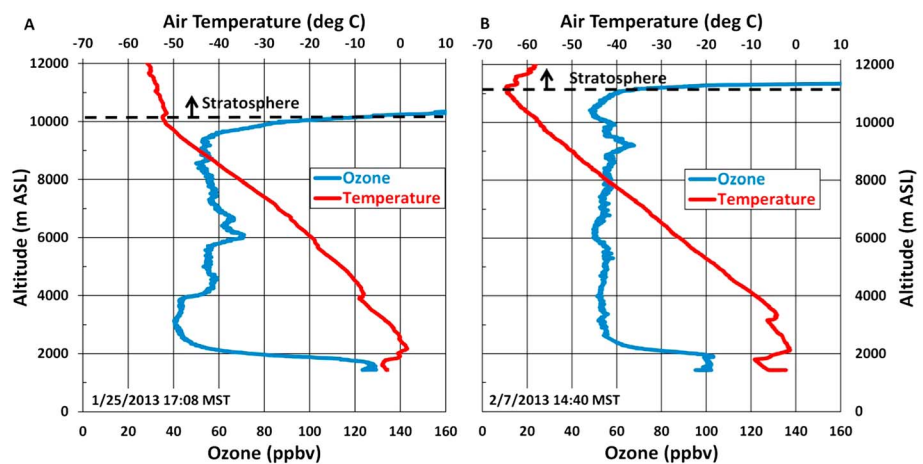


**Figure 9.** Free-flying ozonesonde profiles at Ouray on 25 January and 7 February. In these profiles, high photochemical ozone-mixing ratios are confined to the lowest 200 m agl capped by a sharp temperature inversion. Throughout the troposphere the mixing ratios were in the range 50–60 ppbv that is normal for this latitude and time of year. Only when the balloons entered the stratosphere did ozone-mixing ratios exceed those measured in the lower 200 m agl.

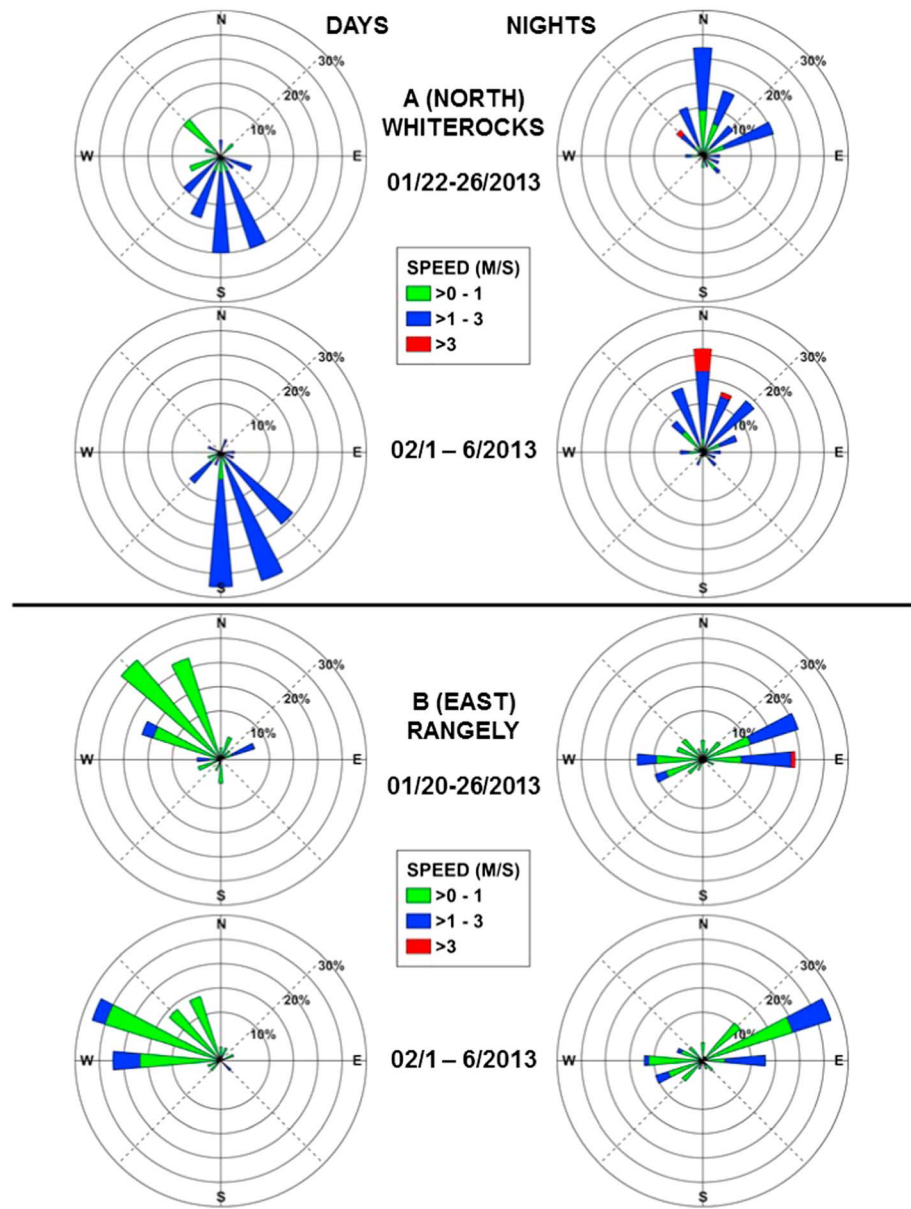


**Figure 10.** Wind roses for ozone measurement sites around the edge of the Uinta Basin. Wind roses for day (1000–1500 MST) and night (1600–0900 MST) showing persistent daytime upslope and nighttime downslope winds during the 22–26 January and 1–6 February ozone production events in all four cardinal-direction slopes in the Uinta Basin.

200 m agl and attained a peak of 13.0 ppbv/h in the 50 and 100 m layers. At Fantasy Canyon on 6 February, the growth rate was 11.1 ppbv/h or greater at all heights and reached 13.2 ppbv/h at the 100 m height (Table 2).

To calculate the overnight ozone loss rate, the ozone-mixing ratio at the beginning of the subsequent day was subtracted from the peak of the prior day and divided by the intervening hours. For consistency in calculating the ozone decrease rates, data for the 250 and 200 m levels were excluded as those levels were often influenced by lower ozone air from above as the depth of the cold pool decreased in the evening. The hourly averaged ozone loss rates are presented in Table 3. Ozone-mixing ratios decreased relatively uniformly through the cold-pool layer ranging between  $-2.5$  and  $-0.8$  ppbv/h at Ouray and  $-2.7$  ppbv and  $-1.0$  ppbv/h at Fantasy Canyon. The diurnal cycle observed at the surface monitoring sites (Figure 3) was essentially present throughout the cold-pool layer.

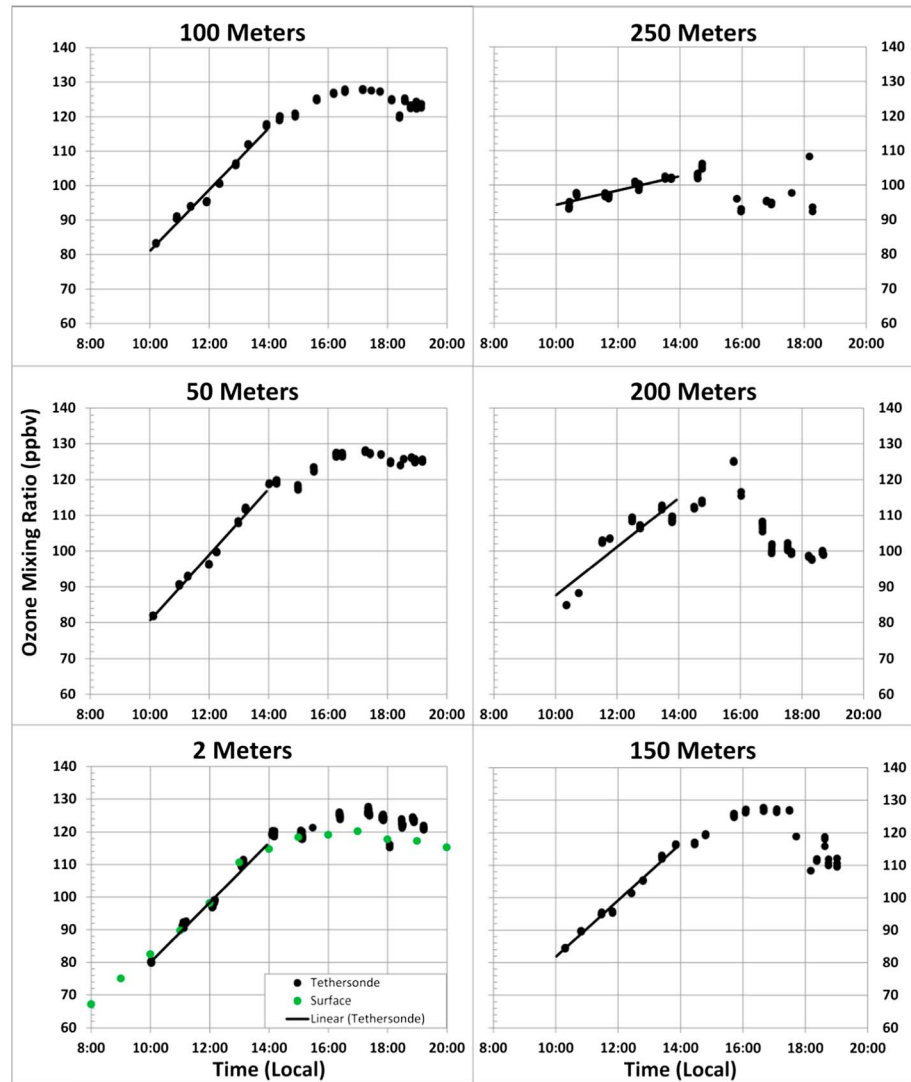


**Figure 11.** Ozone growth rates at Ouray determined from the slope of the best fit to the measurements between 1000 and 1400 MST. Ozone-mixing ratios at Ouray plotted at 50 m height intervals from 2 m above the surface to 250 m for each profile for each day. Ozone-mixing ratios from the surface monitor at Ouray are plotted in green at the 2 m level.

### 3.8. NO<sub>x</sub> in the Bonanza Power Plant Plume Related to the Cold Pool

The coal-fired Bonanza power plant located in the eastern portion of the basin released close to 700 short tons of NO<sub>x</sub> in January and 1200 tons in February 2013 [Bonanza NO<sub>x</sub> Releases, 2013]. This NO<sub>x</sub> would be an ozone precursor if it was entering the cold pool. The top of the exhaust stack of the power plant is at 1716 m asl (~150 magl), and the exhaust plume generally rose an additional two to three stack heights (Figure S7) before usually leveling off at 1900–2200 m asl, except on 14–15 February when the base of the plume appeared to be at 1750 m asl near midnight as seen in Figure 8, where the plumes are identified by the purple colored plumes outlined in the dark bordered boxes.

Representative ozone profiles from Horse Pool tethersondes downwind of the power plant that passed through the plume on 2 and 14 February (Figure 12) show plume heights to be centered at ~1900 and ~1850 m asl, respectively. On 2 February within the cold pool (1620 m and below), ozone-mixing ratios were up to ~110 ppbv and 60 ppbv in the free troposphere above the plume. On 14 February, ozone peaked at just less than 120 ppbv at 1600 m asl in the cold pool and was 60 ppbv above the plume.

**Table 2.** Tethersonde Hourly Average Ozone Growth Rates at the Surface (2 m) and in 50 m Vertical Segments at Ouray and Fantasy Canyon, 31 January to 6 February 2013<sup>a</sup>

Level (m)	1/31/2013	2/1/2013	2/2/2013	2/3/2013	2/4/2013	2/5/2013	2/6/2013
<i>Ouray Growth Rates (ppbv/h)</i>							
2	6.0	8.3	4.4	6.1	7.0	9.2	11.2
50	4.0	7.7	4.5	5.9	6.5	9.2	13.0
100	3.8	7.3	4.3	4.9	6.1	8.9	13.0
150	3.6	7.3	5.7	1.9	4.1	8.7	12.6
200	2.9	2.6	5.8	-0.9	3.0	6.8	11.9
250	1.8	5.2	4.5	0.5	3.8	2.1	N/A
<i>Fantasy Canyon Growth Rates (ppbv/h)</i>							
2	9.0	9.0	6.9	7.4	7.6	9.3	11.6
50	8.6	8.2	6.6	7.2	6.8	8.7	11.6
100	10.3	7.1	6.5	1.7	6.2	10.7	13.2
150	3.3	6.2	6.8	0.8	4.0	7.6	11.3
200	3.8	6.9	7.7	2.4	2.2	12.0	11.1
250	2.0	3.7	8.8	3.1	4.1	7.7	N/A

<sup>a</sup>Between 40 and 70 data points were averaged for each growth rate value presented in the table.

#### 4. Discussion and Conclusions

The contrasting UB wintertime ozone production between 2012 (none) and 2013 (large) was controlled mainly by snow cover and the associated development of a persistent cold pool topped by a strong temperature inversion. The 2013 snow cover and meteorological conditions in the UB mirror conditions that produced wintertime ozone production were first observed in the Upper Green River Basin, Wyoming [Schnell *et al.*, 2009]. Other studies [Karion *et al.*, 2013; Helmig *et al.*, 2014; Warneke *et al.*, 2014] show that the main source of the ozone precursors in the Uintah Basin is related to natural gas operations.

The day-to-day buildup of the nighttime minimum ozone values and daytime maxima during an ozone production event implies that the nightly ozone loss does not compensate for the daytime production. Ozone production on a given day is built on the previous day's ozone concentration until an episode concluded with the sudden (as on 27 January) or more gradual (as on 7–10 February) scouring of the basin by transport of cleaner air into the basin.

The net rate of daytime ozone production during the events was somewhat variable but generally in the range of 5–11 ppbv/h throughout the cold pool (Table 2). Peak hourly ozone production of 13.2 ppbv/h was measured at Fantasy Canyon on 6 February. Ozone losses during the night were generally in the 1–2 ppbv/h range at heights between 2 and 150 m (Table 3). In the City of Vernal (Figures 3 and 4), the nighttime ozone decrease was much greater than at any other surface ozone site. This nighttime decrease was probably due to ozone titration by NO emissions from vehicle exhaust owing to 24 h per day heavy vehicle traffic serving the oil and gas industry. The tethersonde ozone and temperature measurements (Figures 4, 6, and 8) and a vehicle transect

**Table 3.** Hourly Average Ozone Loss Rates at the Surface (2 m) and in 50 m Vertical Segments at Ouray and Fantasy Canyon, 1 January to 6 February 2013<sup>a</sup>

Level (m)	1/31 to 2/1	2/1-2/2	2/2-2/3	2/3-2/4	2/4-2/5	2/5-2/6
<i>Ouray Loss Rates (ppbv/h)</i>						
2 m	-2.5	-1.7	-2.4	-2.1	-0.9	-1.6
50 m	-2.5	-1.8	-2.2	-2.1	-0.8	-1.6
100 m	-2.3	-2.0	-1.6	-1.8	-0.9	-1.4
150 m	-2.0	-1.8	-1.3	-1.4	-0.8	-1.2
<i>Fantasy Canyon Loss Rates (ppbv/h)</i>						
2 m	-2.4	-2.6	-2.1	-2.3	-1.8	-1.8
50 m	-2.3	-2.1	-1.5	-2.7	-1.6	-1.8
100 m	-2.4	-2.0	-1.0	-1.9	-1.7	-1.2
150 m	-1.7	-2.3	-1.2	-2.8	-2.0	-1.8

<sup>a</sup>Between 40 and 70 data points were averaged for each growth rate value presented in the table.

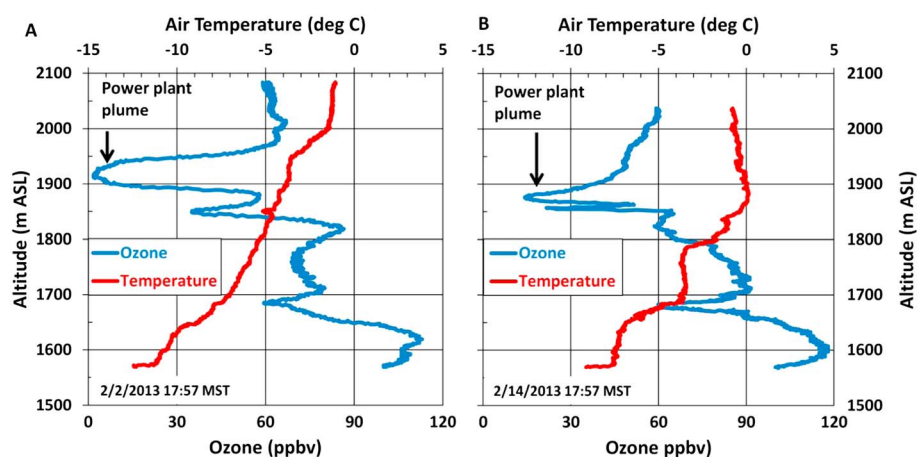


**Figure 12.** Ozone profiles through the Bonanza power plant plume. Tethersonde ozone and temperature profiles on 2 and 14 February at Horse Pool. When the sondes intercepted the Bonanza power plant exhaust plume at 1900–1950 m asl and 1850–1900 m asl on 2 and 14 February, respectively, they “indicated” low ozone values due to interference with  $\text{SO}_2$  and  $\text{NO}$  titration of ozone. Note the decrease in the near-surface ozone concentrations that occur late in the day when ozone destruction processes are greater than ozone production.

up the south side of the basin (Figure 5) confirm that the cold pool did not extend high enough to spill over the basin rims, but did spread up the White River valley to Rangely, CO (elevation 1648 m asl) and north into the Dinosaur National Monument. The elevated ozone was periodically flushed out of the basin with the passage of frontal systems bringing low ozone air into the basin as shown in Figures 3 and 6–8 (see also Figure S4).

The sequence of ozone profiles from three locations in the basin (Figure 6), the ozone time/height cross sections (Figures 7 and 8), and ozone-mixing ratios at fixed altitudes (Figure 11) all show that ozone production during daytime occurs generally uniformly throughout the vertical extent of the cold-pool layer. This occurs both near the beginning of an episode when the early-morning mixing ratios are relatively low, for instance, on 30 January ( $\sim 40$  ppbv) and at the peak of an episode such as on 6 February when early-morning mixing ratios were  $\sim 100$  ppbv. Within the cold pool, most daytime temperature profiles were near isothermal, with temperatures below  $0^\circ\text{C}$  and generally no more than  $1\text{--}2^\circ\text{C}$  warmer at the surface, but up to  $8\text{--}10^\circ\text{C}$  warmer above the top of the cold pool, as seen for the 30 January to 6 February event (Figure 6).

The top of the cold pools in the 1650–1750 m asl range was at heights well below the rim of the UB (Figure 1) such that the oil and gas operation effluents and the resulting photochemically produced ozone were generally constrained in a relatively shallow layer within the approximate central 50% of the basin (Figure 1b). Based upon the hundreds of tethersonde profiles and mobile van observations, the top of the cold-pool ozone production layer was observed to be essentially level in altitude across the basin. The upper boundary height of the cold pool was independent of the underlying surface elevations and river valleys.

Horizontal surface wind speed and direction measurements throughout the basin show that air moves toward the basin edges as a result of daytime heating on the basin slopes (Figures 10 and S6). When heating is absent (nighttime), cooling temperatures produce downslope drainage directed toward the lower portions of the basin. These diurnal winds occasionally mix ozone precursors and ozone to the outer reaches of the basin in a pattern documented for similar topographically confined settings [Whiteman *et al.*, 1989; Lehner *et al.*, 2011]. This accounts for the occasional elevated ozone concentrations on the outskirts of the basin.

The tethersonde penetrations of the Bonanza power plant plume (Figures 8 and 12) show that the effluents from the smoke stack are released above the top of the cold pool during the period of the ozone production events described above; therefore,  $\text{NO}_x$  in the warmer air of the power plant plumes does not mix down through the temperature inversion into the much colder cold-pool ozone production layer below. These observations support the preponderance of data showing that the ozone precursors are coming primarily from the oil and gas production operations within the basin and not from the power plant.

## Acknowledgments

Ouray U.S. Fish and Wildlife Service Management at the Ouray National Wildlife Refuge generously provided facilities for tethered operations, and the U.S. Bureau of Land Management allowed access to Fantasy Canyon. Richard Payton, USEPA Region 8, Denver, CO, was especially helpful in providing surface ozone, NO, and wind data for the Uinta Basin in a fast, professional and congenial manner. Uinta Basin EPA data are available at <http://www2.epa.gov/aqs> and <http://ampd.epa.gov/ampd/>. NOAA data for the Uinta Basin study are available at <ftp://aftp.cmdl.noaa.gov/data/ozwv/>. Ozonesonde/Field Projects/Uintah/UINTAH 2013/. Wyoming ozone data are available at <http://deq.wyoming.gov/aqd/winter-ozone/>. Utah gas and oil data are available at <http://oilgas.ogm.utah.gov/> and <http://www.deq.utah.gov/locations/U/uintahbasin/ozone/overview.htm>. R.C.S. and B.J.J. contributed to conception and design. B.J.J., P.C., C.S., E.H., A.J., D.H., R.A., J.W., R.A., P.B., C.R.T., J.E., J.H., A.C., J.-H.P., and R.C.S. contributed to the acquisition of data. R.C.S., S.J.O., D.H., G.P., B.J.J., R.A., C.S., P.C., and E.H. contributed to analysis and interpretation of data. R.C.S., S.J.O., D.H., and G.P. contributed to drafting the article or revising it critically for important intellectual content. R.C.S., B.J.J., S.J.O., P.C., C.S., E.H., A.J., D.H., G.P., J.W., P.B., C.R.T., J.E., J.H., A.C., and J.-H.P. contributed to the final approval of the version to be published. Funding was provided by the NOAA Climate Program Office. Additional funding and in-kind support for the 2013 Uinta Basin Ozone Study was provided by the Uintah Impact Mitigation Special Service District (UIMSSD), Western Energy Alliance, QEP Resources, Inc., Bureau of Land Management (BLM), Environmental Protection Agency (EPA), Utah Department of Environmental Quality (UDEQ) and Utah Science Technology and Research Initiative (USTAR), and Utah School and Institutional Trust Lands Administration (SITLA). All NOAA data used in this project, including graphical plotting routines, are available through the NOAA/ESRL Global Monitoring Division <ftp://aftp.cmdl.noaa.gov/data/ozwv/Ozonesonde/FieldProjects/Uintah/UINTAH 2013/>. If data access is not available to a requestor, contact [russell.c.schnell@noaa.gov](mailto:russell.c.schnell@noaa.gov). The authors declare no competing interests.

## References

- Ahmadov, R., et al. (2015), Understanding high wintertime ozone in oil and natural gas producing region of the western U.S., *Atmos. Chem. Phys.*, *15*, 411–429, doi:10.5194/acp-15-411.
- Baker, K. R., H. Simon, and J. T. Kelly (2011), Challenges to modeling “cold pool” meteorology associated with high pollution episodes, *Environ. Sci. Technol.*, *45*(17), 7118–7119, doi:10.1021/es202705v.
- Bonanza NO<sub>x</sub> releases (2013), [Available at <http://ampd.epa.gov/ampd/>]
- Edwards, P. M., et al. (2013), Ozone photochemistry in and oil and natural gas extraction region during winter: Simulations of a snow-free season in the Uintah Basin, Utah, *Atmos. Chem. Phys.*, *13*, 8955–8971, doi:10.5194/acp-13-8955-2013.
- Edwards, P. M., et al. (2014), High winter ozone generated by carbonyl photolysis in a shale gas and oil producing region, *Nature*, *514*, 351–354, doi:10.1038/nature13767.
- Helmig, D., C. R. Thompson, J. Evans, P. Boylan, J. Hueber, and J. H. Park (2014), Highly elevated levels of volatile organic compounds in the Uintah Basin, Utah, *Environ. Sci. Technol.*, *48*, 4707–4715, doi:10.1021/es405046r.
- Johnson, B. J., D. Helmig, and S. J. Oltmans (2008), Validation of ozone measurements from a tethered balloon sampling platform at South Pole Station in December 2003, *Atmos. Environ.*, *42*, 2780–2787, doi:10.1016/j.atmosenv.2007.03.043.
- Karion, A., et al. (2013), Methane emissions estimate from airborne measurements over a western United States natural gas field, *Geophys. Res. Lett.*, *40*, 4393–4397, doi:10.1002/grl.50811.
- Lehner, M., C. D. Whiteman, and S. W. Hoch (2011), Diurnal cycle of thermally driven cross-basin winds in Arizona’s Meteor Crater, *J. Appl. Meteorol. Climatol.*, *50*, 729–743, doi:10.1175/2010AMC2520.1.
- Luria, M., R. J. Valente, R. L. Tanner, N. V. Gillani, R. E. Imhoff, S. F. Mueller, and J. F. Meagher (1999), The evolution of photochemical smog in a power plant plume, *Atmos. Environ.*, *33*(18), 3023–3036, doi:10.1016/S1352-2310(99)00072-2.
- Luria, M., R. E. Imhoff, R. J. Valente, and R. L. Tanner (2003), Ozone yields and production efficiencies in a large power plant plume, *Atmos. Environ.*, *37*, 3593–3603, doi:10.1016/s1352-2310(03)00342.
- Lyman, S., and H. Shorthill (2013), Final report: 2012 Uintah Basin Winter Ozone and Air Quality Study. Doc. CRD13-320.32, Commercialization and Regional Development, Utah State Univ., 1 February. [Available at [http://rd.usu.edu/files/uploads/ubos\\_2011-12\\_final\\_report.pdf](http://rd.usu.edu/files/uploads/ubos_2011-12_final_report.pdf)]
- Lyman, S., and T. Tran (2015), Inversion structure and winter ozone distribution in the Uintah Basin, Utah, USA, *Atmos. Environ.*, *123*, 156–165, doi:10.1016/j.atmosenv.2015.10.067.
- Neemann, E. M., E. T. Crosman, J. D. Horel, and L. Aver (2015), Simulations of a cold-air pool associated with elevated wintertime ozone in the Uintah Basin, Utah, *Atmos. Chem. Phys.*, *15*, 135–151, doi:10.5194/acp-15-1135-2015.
- Oltmans, S., R. Schnell, B. Johnson, G. Pétron, T. Mefford, and R. Neely III (2014), Anatomy of wintertime ozone production associated with oil and gas extraction activity in Wyoming and Utah, *Elementa*, *2*, 1–15, doi:10.12952/journal.elementa.000024.
- Schenkel, A., and B. Broder (1982), Interference of some trace gases with ozone measurements by the KI method, *Atmos. Environ.*, *16*, 2187–2190, doi:10.1016/00046981(82)90289x.
- Schnell, R. C., S. J. Oltmans, R. R. Neely III, M. S. Endres, J. V. Molenar, and A. B. White (2009), Rapid photochemical production of ozone at high concentrations in a rural site during winter, *Nat. Geosci.*, *2*, 120–122, doi:10.1038/ngeo415.
- Smit, H. G. J., et al. (2007), Assessment of the performance of ECC-ozonesondes under quasi-flight conditions in the environmental simulation chamber: Insights from the Juelich Ozone Sonde Intercomparison Experiment (JOSIE), *J. Geophys. Res.*, *112*, D19306, doi:10.1029/2006JD007308.
- Stoekenius, T., and D. McNally (Eds.) (2014), Final report: 2013 Uintah Basin Winter Ozone Study can be found at. [Available at <http://www.deq.utah.gov/locations/uintahbasin/studies/UBOS-2013.htm>]
- Uinta Basin Mobile Measurements (2016), see [ftp://aftp.cmdl.noaa.gov/data/ozwv/Ozonesonde/Field Projects/Uintah/UINTAH 2013/6\\_MobileVan\\_Ozonesonde/](ftp://aftp.cmdl.noaa.gov/data/ozwv/Ozonesonde/Field Projects/Uintah/UINTAH 2013/6_MobileVan_Ozonesonde/)
- Utah DEQ (2016) see <http://www.deq.utah.gov/locations/U/uintahbasin/ozone/overview.htm>
- Utah Oil and Gas Program (2015) see <http://oilgas.ogm.utah.gov/>
- Warneke, C., et al. (2014), Volatile organic compound emissions from the oil and natural gas industry in the Uinta Basin, Utah: Point sources compared to ambient air composition, *Atmos. Chem. Phys.*, *14*, 10,977–10,988, doi:10.5194/acp-14-10977-2014.
- Whiteman, C. D., K. J. Allwine, L. J. Fritschen, M. O. Orgill, and J. R. Simpson (1989), Deep valley radiation and surface energy budget microclimates Part II: Energy budget, *J. Appl. Meteorol.*, *28*, 427–437.
- Wyoming DEQ (2016) see <http://deq.wyoming.gov/aqd/winter-ozone/>